

OPTIMIZED UAV TRAJECTORY PLANNING FOR ACCURATE VICTIMS LOCALIZATION IN POST DISASTER ENVIRONMENT

JIANFENG CHE^{1,2}, YONGYUE ZHANG¹,
SWEE KING PHANG^{1,*}, AFIZAN AZMAN³

¹School of Engineering, Taylor's University, Subang Jaya, Malaysia

²Department of Intelligent Manufacturing, Chengde
College of Applied Technology, Chengde, China

³School of Computer Science, Taylor's University, Subang Jaya, Malaysia

*Corresponding author: sweeking.phang@taylors.edu.my

Abstract

This paper presents an advanced UAV-based system for disaster victim localization, integrating the Ray Tracing model and Weighted Least Squares (WLS) method to enhance the accuracy of RSSI-based distance measurements. The disaster area is modelled by dividing it into a grid, with adaptive waypoints selected using the adaptive Particle Swarm Optimization (APSO) algorithm. The UAV trajectory is optimized using the RRT* algorithm, ensuring efficient coverage with minimized flight costs. Simulation results demonstrate that the proposed system accurately locates disaster victims with localization errors within 5 meters. The RRT* algorithm provides a smoother and more efficient flight path compared to the Nearest Neighbour algorithm, reducing energy consumption and improving rescue operation speed. This integrated approach significantly enhances UAV-based disaster response efforts, ensuring timely and precise victim localization.

Keywords: Digital integrated cities, Path planning, Unmanned aerial vehicles.

1. Introduction

Earthquakes are one of the most destructive natural disasters, posing a significant threat to human life and property. Earthquakes can cause building collapse, infrastructure damage, and communication interruptions, thus requiring rapid and effective post disaster response [1].

In recent years, unmanned aerial vehicles (UAVs) have become an important tool in disaster relief. Drones can conduct aerial reconnaissance, assess losses, generate detailed maps of disaster areas, and transport medical supplies and food to people who have been cut off by traditional supply lines [2]. Drones equipped with cutting-edge imaging technology can capture high-definition images and videos, helping emergency teams make informed decisions. For example, thermal imaging cameras can detect the thermal signals of survivors, while LIDAR sensors generate three-dimensional maps to help rescue personnel navigate through the ruins [3].

The research topic of unmanned aerial vehicles in disaster relief has long been a subject of extensive scholarly interest. Qi et al. [4] presents a study on the development and application of a search and rescue rotary-wing unmanned aerial vehicle (SR-RUAV) system, focusing on its use in post-earthquake response and evaluation, particularly during the Lushan 7.0 earthquake in China. Valarmathi et al. [5] employed the YOLOv3 algorithm for human detection and action recognition in disaster scenarios, showcasing the integration of machine learning, cloud computing, and IoT for enhanced disaster management.

Saif et al. [6] proposed a collaboration model between multi-UAV and SAR teams to extend communication services over larger disaster areas, demonstrating improved coverage and efficiency with increased UAV elevation angles. Enhancing communication and collaboration frameworks is essential for the success of SAR operations. Khalil et al. [7] presented a UAV-swarm-communication model using machine learning for SAR applications, focusing on the integration of UAV communications with space and terrestrial networks. Alhaqbani et al. [8] proposed a fish-inspired algorithm for multi-UAV task allocation in SAR missions, demonstrating superior performance in mean rescue time and survivor percentage compared to other paradigms.

The most critical aspect of disaster response is to quickly rescue trapped or injured individuals. Accurately locating survivors in chaos and destruction is crucial. Especially in urban areas, buildings may collapse into complex ruins, and accurate positioning is crucial for effective command and rescue. This task requires the integration of multiple technologies to overcome the challenges posed by post disaster environments. Oh and Han [9] described a smart search system for autonomous UAVs designed to locate and approach distressed individuals without ground control, employing a genetic-based localization algorithm validated in real-world test fields. Dong et al. [10] developed a real-time survivor detection system using UAVs and deep convolutional neural networks, addressing the challenges of limited computing capacity and small datasets for SAR missions.

Identifying disaster victims in earthquakes faces many difficulties. Chaotic conditions, fragmentation, and damaged communication networks may render traditional positioning methods ineffective. To help drones effectively locate disaster victims, various methods have been explored, including GPS, WiFi and cellular signals, as well as infrared and optical cameras [11]. Although GPS

provides high accuracy in open spaces, its performance is poor in indoor or densely constructed areas. Wi-Fi and cellular signals provide useful data but may be unreliable in the event of infrastructure damage. Visual methods are effective under clear conditions, but limited in smoke, dust, or darkness.

The Integrated Received Signal Strength (IRSS) technology has shown hope in improving positioning accuracy. By analysing the changes in signal strength received by drones, IRSS can estimate the location of signal sources, making it a reliable method for detecting survivors [12]. This technology has proven its effectiveness in various environments and demonstrated its ability to perform reliable localization in complex environments.

Despite the progress made in IRSS technology, there are still challenges such as multipath effects, signal attenuation, and environmental barriers that can affect the accuracy of signal localization [13, 14]. This manuscript proposes using an improved ray tracing model to improve the positioning accuracy based on IRSS. In addition, we have introduced an optimized path planning algorithm to ensure comprehensive coverage of drones, thereby further improving the effectiveness of rescue operations. By integrating these methods, we aim to overcome the limitations of current methods and provide more reliable disaster response solutions.

2. Methods

2.1. Overview

This study aims to enhance the methods for UAV-based localization and path planning in earthquake disaster rescue operations. First, we model the disaster area and divide it into a 20×30 grid. This division facilitates a detailed analysis of the disaster situation in each region. Based on actual disaster conditions, we classify the disaster levels for each grid cell, with darker colours representing more severe areas. Simultaneously, we collect Received Signal Strength Indicators (RSSI) from mobile devices detected among the affected population.

Next, we use the Adaptive Particle Swarm Optimization (APSO) algorithm to select the optimal hovering points. This ensures that UAVs can monitor and collect the required RSSI readings for each grid cell from these positions. The APSO algorithm simulates the movement of a swarm of particles in the search space to find the global optimum, thereby determining the minimal number of hovering points.

After identifying the necessary hovering grid positions, we convert the path planning problem into a Traveling Salesman Problem (TSP) and solve it using the F-RRT* path planning algorithm. The F-RRT* algorithm combines heuristic search and cost functions to efficiently compute the optimal path from the starting point to all scanning points, thus enhancing coverage efficiency and path planning accuracy. During the UAV flight, we dynamically adjust the flight path by receiving and analysing RSSI data in real time. The F-RRT* algorithm updates the path cost and heuristic estimates in real time, optimizing the flight trajectory to adapt to dynamically changing environments and signal conditions.

Finally, we employ the Ray Tracing model and the Weighted Least Squares (WLS) method for RSSI-based distance detection and personnel localization. The Ray Tracing model simulates the actual propagation path of signals, improving the accuracy of signal strength prediction. The WLS method uses multiple RSSI

measurements and detailed signal propagation simulations to accurately locate disaster victims. This combined approach offers higher localization accuracy and reliability compared to traditional log-normal shadowing path loss models and trilateration methods.

In summary, this methodology is summarised in Fig. 1. It improves the efficiency and accuracy of UAV-based localization and rescue operations in disaster environments through an enhanced signal strength prediction model and optimized path planning algorithms. Our approach demonstrates good adaptability and reliability in complex disaster scenarios, providing more effective technical support for disaster response.

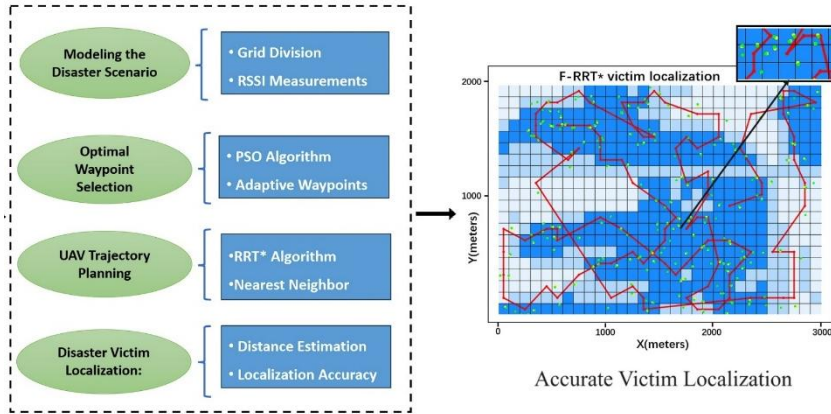


Fig. 1. System framework to accurately localize victim.

2.2. Modelling earthquake scenarios

This section utilizes aerial imagery from the Wenchuan Earthquake in China as a case example to model a disaster scenario. In the aftermath of the earthquake, the communication infrastructure is assumed to be severely damaged, leaving survivors potentially trapped under debris and carrying mobile devices that have lost their wireless connectivity. In such a dire context, the swift and accurate localization of survivors is paramount for effective rescue operations.

To achieve this objective, a systematic approach is implemented to model and segment the affected area. The disaster-stricken region is divided into a grid consisting of 30 rows and 55 columns, with each grid cell measuring 5 meters on each side. Each grid cell is assigned a different colour depth to represent the severity of the damage in that area. Darker colours indicate more severe damage, and these areas, consequently, require a higher number of RSSI (Received Signal Strength Indicator) readings to enhance localization accuracy.

As illustrated in Fig. 2(a) represents the aerial photograph of the 2008 Wenchuan Earthquake in China, while Fig. 2(b) shows the grid modelling performed on the affected area. From the figure, it can be observed that regions such as farmland and mountains are designated as low disaster levels, whereas densely populated areas and collapsed buildings are assigned high disaster levels, with a total of five levels. Different levels of areas require varying levels of

Received Signal Strength Indicator (RSSI) signals. Each grid is a square region with a side length of 5 meters, and the required RSSI signal for each grid is denoted by K , where i represents the i -th row and j represents the j -th column. This grid-based modelling approach enables refined management of the disaster area.

By dividing the entire affected region into multiple small grids, we can more accurately assess the disaster situation of each grid cell and formulate corresponding rescue strategies accordingly. Additionally, the grid-based approach helps to enhance localization accuracy. In disaster scenarios, traditional GPS localization may fail due to environmental interference. By meticulously collecting RSSI readings for each grid cell, we can utilize wireless signal strength to estimate device locations, thereby achieving higher localization accuracy.

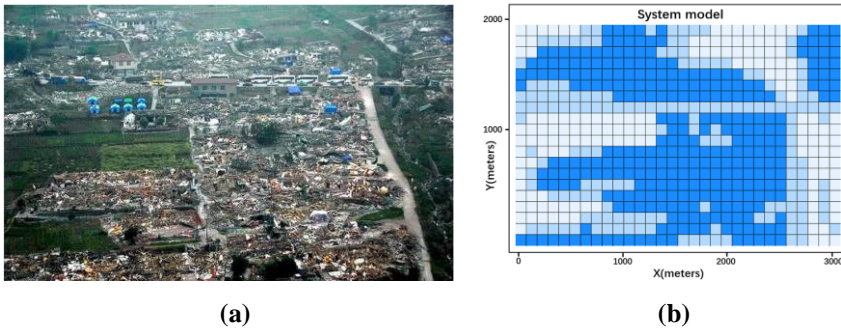


Fig. 2. System model diagram (a) Aerial photo of the 2008 Wenchuan earthquake; (b) Grid model constructed based on disaster level.

2.3. Determining UAV waypoints

This section will determine the optimal waypoint for drones to ensure the full positioning of the affected population in the disaster area, while minimizing flight time and resource consumption.

Firstly, based on the disaster model, each grid unit represents a specific area that needs to be scanned. Each grid unit sets different receiving RSSI readings based on the severity of the disaster. The higher the disaster level, the more RSSI signals need to be received. Due to the constraints of complete coverage and optimal flight path in the task objective, RSSI signals from all regions are received with the minimum number of scanning points. This task has the characteristic of combinatorial optimization, which can convert determining the optimal waypoint of the drone into a Set Cover Problem, the problem of SCP belongs to a variant of NP Hard problem. To solve this problem, advanced optimization techniques are needed to find an approximate optimal solution.

This study adopts the adaptive particle swarm optimization (APSO) algorithm to solve this problem. APSO introduces dynamic adjustment mechanisms for the PSO parameters, specifically tailored to address the unique challenges of UAV waypoint optimization in disaster scenarios. The key features of APSO include dynamic inertia weight, adaptive learning factors, mutation operations, and local search mechanisms. The specific formulas for the Adaptive Particle Swarm Optimization (APSO) algorithm are as follows:

Velocity update equation:

$$V_i(t+1) = w(t)V_i(t) + c_1r_1(p_i - x_i(t)) + c_2r_2(g - x_i(t)) \quad (1)$$

where $V_i(t+1)$ represents the velocity of particle i at time $t+1$, $w(t)$ is the dynamic inertia weight, c_1 and c_2 are the adaptive learning factors controlling the tendency of the particle to move towards its individual best position and the global best position, respectively, r_1 and r_2 are random numbers in the range $[0, 1]$, p_i represents the individual best position of particle i , and g represents the global best position of all particles.

Position update equation:

$$x_i(t+1) = x_i(t) + V_i(t+1) \quad (2)$$

where $x_i(t+1)$ represents the position of particle i at time $t+1$, and $x_i(t)$ represents the position of particle i at time t .

Individual Best Position Update Equation:

$$p_i = \begin{cases} x_i(t+1) & \text{if } f(x_i(t+1)) < f(p_i) \\ p_i & \text{otherwise} \end{cases} \quad (3)$$

where $f(x_i(t+1))$ is the fitness function value of particle i at position $x_i(t+1)$.

Global Best Position Update Equation:

$$g = \min(f(p_i)) \quad (4)$$

where g represents the global best position. Constraint Conditions: Each grid cell must be covered by at least one scanning point:

$$\sum_{j=1}^n y_{ij} \geq 1, \forall i \in \{1, 2, \dots, m\} \quad (5)$$

where y_{ij} indicates whether scanning point j covers grid cell i , m represents the total number of grid cells, and n represents the total number of scanning points.

High-disaster-level areas require more RSSI readings, resulting in a higher density of scanning points:

$$K_{ij} = \left\lceil \frac{D_{ij}}{r_s} \right\rceil \quad (6)$$

where K_{ij} represents the required RSSI readings for grid cell (i, j) , D_{ij} represents the disaster level, and r_s is the signal coverage radius of each scanning point.

2.4. UAV path planning

Given the consideration of flight costs associated with UAVs, it is imperative to identify a flight path with the lowest possible expenses. Hence, this paper employs the F-RRT* algorithm as the chosen method for path planning.

F-RRT* is an improved version of the RRT* (Rapidly-exploring Random Trees Star) algorithm. The main idea of F-RRT* is that in each iteration, instead of just considering the nearest node to expand, a set of nearest-neighboring nodes are considered and the best of them are selected for expansion [15]. In this way, the algorithm can explore the configuration space faster and find high-quality paths earlier.

Compared to the standard RRT* algorithm, F-RRT* exhibits a faster convergence rate. This indicates that it can find optimal or near-optimal paths in fewer iterations. Additionally, the paths generated by F-RRT* tend to be smoother and more direct, making it particularly suitable for applications where efficiency and safety are of paramount importance, such as unmanned aerial vehicle flight planning. The specific flow of the F-RRT* algorithm is shown in Table 1.

Table 1. Specific description of each step of the F-RRT* algorithm.

Step	Process	Description
1	Initialization	Start with an initial node q_{start} , and define the goal node q_{goal} .
2	Sampling	In each iteration, randomly sample a point q_{rand} in the search space.
3	Nearest Node	Find the node $q_{nearest}$ in the tree that is closest to q_{rand} .
4	Steering	Generate a new node q_{new} by moving from $q_{nearest}$ towards q_{rand} but within a maximum distance, Delta q.
5	Obstacle Check	Ensure the path segment between $q_{nearest}$ and q_{new} is free from collisions.
6	Cost Calculation	Compute the cost to reach q_{new} from q_{start} via $q_{nearest}$
7	Rewiring	Check nodes in the vicinity of q_{new} and see if it's more cost-effective to reach them via q_{new} . Update connections accordingly.
8	Goal Check	If q_{new} is close enough to q_{goal} and a direct connection is possible, link them.
9	Completion	Once the goal is reached or after a predefined number of iterations, the algorithm concludes. The optimal path can be traced back from q_{goal} to q_{start} .

2.5. RSSI-based distance detection and personnel localization

The utilization of a singular UAV for surveillance purposes in disaster zones entails a perpetual motion strategy aimed at gathering Received Signal Strength Indication (RSSI) data from diverse sites. This UAV adheres to a predetermined flight trajectory spanning the entirety of the impacted region to guarantee consistent data acquisition. Subsequently, a ray-tracing model is employed to compute the transmission routes of signals, accounting for intricate occurrences like reflection, refraction, and diffraction. This theoretical framework contributes to elucidating the transmission behavior of signals within the surroundings, their interaction with impediments, and the attenuation of signal potency over distances.

In this study, we used a ray tracing model and weighted least squares (WLS) method for distance detection and personnel localization based on RSSI. The ray tracing model can simulate the actual propagation path of signals and improve the accuracy of signal strength prediction. The following is the specific work process:

$$PL(d) = PL(d_0) + 10n \log_{10} \left(\frac{d}{d_0} \right) + X_{\sigma} \quad (7)$$

where $PL(d)$ is the path loss at distance d , $PL(d_0)$ is the path loss at reference distance d_0 , n is the path-loss exponent, and X_σ is a normal random variable representing shadowing effects.

Based on the Ray Tracing model and the measured RSSI values, we estimate the distance between the UAV and the victims' mobile devices. The distance estimation formula is:

$$d_i = d_0 \cdot 10^{\frac{(RSSI_0 - RSSI_i)}{10 \cdot n}} \quad (8)$$

where d_i is the estimated distance to the i_{th} victim, $RSSI_i$ is the RSSI value from the i_{th} victim, and $RSSI_0$ is the reference RSSI value at distance d_0 .

The accuracy of each RSSI measurement is influenced by the signal-to-noise ratio (SNR). We construct a weighted matrix W based on the SNR, where the weights are inversely proportional to the measurement uncertainties:

$$W_{ii} = \frac{1}{\sigma_i^2} \quad (9)$$

where σ_i is the standard deviation of the i -th measurement.

The Weighted Least Squares (WLS) method is utilized in the estimation of victim positions. This approach involves the minimization of a specific objective function to determine the most accurate position estimates.

$$\hat{\mathbf{p}} = \arg \min \sum_{i=1}^N W_{ii} (d_i - \sqrt{(x_i - x)^2 + (y_i - y)^2})^2 \quad (10)$$

where $\hat{\mathbf{p}} = (x, y, z)$ is the estimated position of the victim, (x_i, y_i, z_i) is the UAV's position at the i_{th} measurement, and d_i is the estimated distance.

By solving the objective function, the two-dimensional coordinates of each trapped individual are obtained. Iteratively update the position estimation until convergence to the minimum error is achieved.

3. Results and Discussion

3.1. Simulation setup

In this section, we present the simulation setup and discuss the results of our disaster victim localization algorithm. To evaluate the performance of the proposed method, we conducted extensive simulations using MATLAB. The UAV was assumed to operate at a fixed altitude of h meters. The UAV's operational radius for victim detection was set to 30 meters, ensuring a comprehensive coverage area around each hover point.

The UAV's speed was configured to 5 meters per second (m/s), a reasonable speed that balances rapid area coverage and stable signal reception for accurate RSSI measurements. The UAV's flight path started from a randomly selected initial position within the disaster area grid. This randomness in the starting point was introduced to simulate real-world scenarios where the UAV may not always have a predefined starting location and needs to adapt to various initial conditions.

At each hover point, the UAV paused for a 10 s to collect the necessary RSSI readings from the mobile devices of the disaster victims. This pausing ensured that the UAV could accurately measure signal strengths and reduce the impact of noise and other environmental factors on the readings.

3.2. UAV waypoint selection results

This section presents the results of selecting optimal UAV waypoints using an adaptive Particle Swarm Optimization (PSO) algorithm to ensure comprehensive coverage of the disaster area. The PSO process begins with an initial random distribution of particles across the grid. Each particle evaluates its fitness based on the number of RSSI measurements it can collect within its coverage radius. The particles iteratively update their positions, moving towards regions with higher fitness values. This adaptive mechanism allows the algorithm to converge on an optimal set of waypoints that ensures comprehensive coverage of the disaster area while prioritizing regions with severe damage, the result is shown in Fig. 3.

As shown in Fig. 3, a total of 98 flight waypoints were generated, marked by red dots. Each waypoint is positioned at the center of the corresponding grid cell. From the figure, it is evident that the generated waypoints cover the entire disaster area. In regions with severe damage, there are more waypoints, reflecting the higher number of required RSSI signal measurements. This distribution of waypoints aligns with the mission's objectives, ensuring that the UAV collects sufficient data to accurately locate victims in the most affected areas.

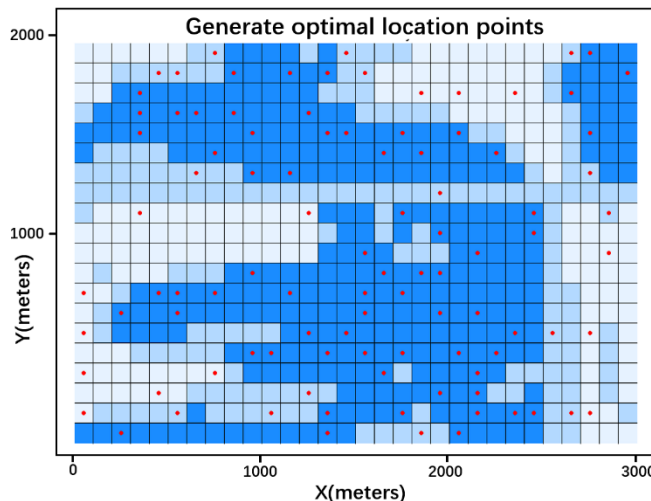


Fig. 3. Generated optimal location points.

3.3. UAV trajectory generation results

In this section, we present the results of UAV trajectory generation using the F-RRT*. The objective is to generate a UAV flight path that passes through all the predetermined waypoints while minimizing the flight cost. To compare the effectiveness of the F-RRT* algorithm, we also utilized the Nearest Neighbour (NN) algorithm. The resulting trajectory paths are shown in Fig. 4.

As depicted in Fig. 4, both algorithms successfully enable the UAV to cruise through all the waypoints. However, the trajectory generated by the proposed F-RRT* algorithm is noticeably smoother. This smoothness translates to a more efficient path, reducing sharp turns and abrupt changes in direction, which are beneficial for maintaining the UAV's stability and energy efficiency.

Figure 5 illustrates the total flight distance covered by the UAV using both the F-RRT* and NN algorithms. It is evident from the figure that the path planned using the F-RRT* algorithm results in a significantly shorter flight distance compared to the NN algorithm. This reduction in flight distance directly correlates to lower energy consumption, thus extending the UAV's operational time and enhancing the speed of rescue missions.

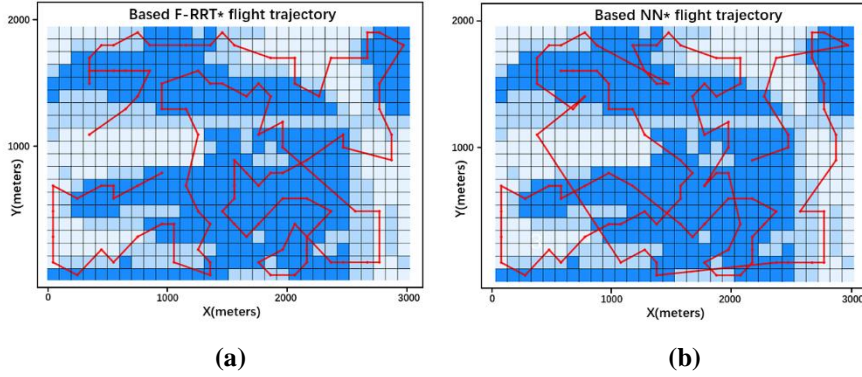


Fig. 4. System model diagram: (a) Trajectory generated using the proposed F-RRT* algorithm; (b) Trajectory generated using the comparative Nearest Neighbour algorithm.

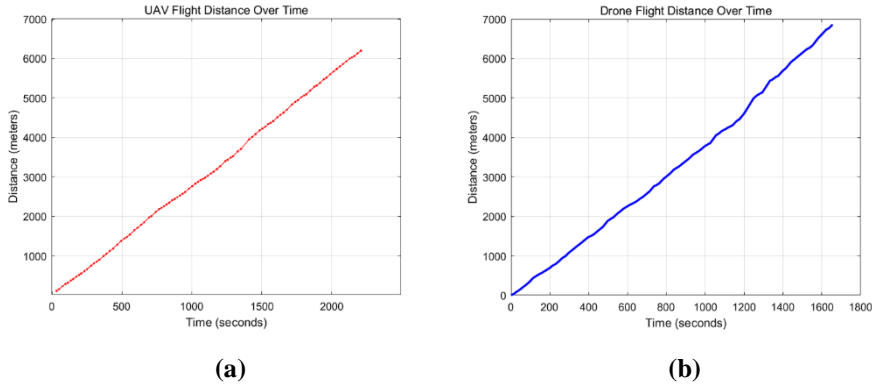


Fig. 5. Comparison result of UAV flight distance: (a) with the proposed F-RRT* path planning algorithm; (b) using the NN path planning algorithm.

3.4. UAV disaster victim localization results

To validate the effectiveness of the proposed localization algorithm, we simulated a scenario with 200 disaster victims, represented by yellow dots in the model. The placement of the disaster victims was based on the severity levels of the affected areas, ensuring a realistic distribution for the simulation.

As shown in Fig. 6, the yellow dots represent the actual positions of the disaster victims, while the green dots indicate the estimated positions calculated by our algorithm. It is evident from the figure that both path planning algorithms, when

combined with our proposed localization method, can accurately pinpoint the victims' locations. This demonstrates the superior performance of our localization system.

Furthermore, Fig. 7 illustrates the localization error of the proposed algorithm. The graph shows that the localization errors are maintained within 5 meters, highlighting the accuracy and reliability of our approach. The results confirm that our system can effectively locate disaster victims in the aftermath of an earthquake, providing critical information for timely rescue operations.

The demonstrated accuracy and efficiency of the proposed system underline its potential to significantly enhance disaster response efforts, ensuring that victims are quickly and precisely located, thus improving the overall effectiveness of the rescue missions.

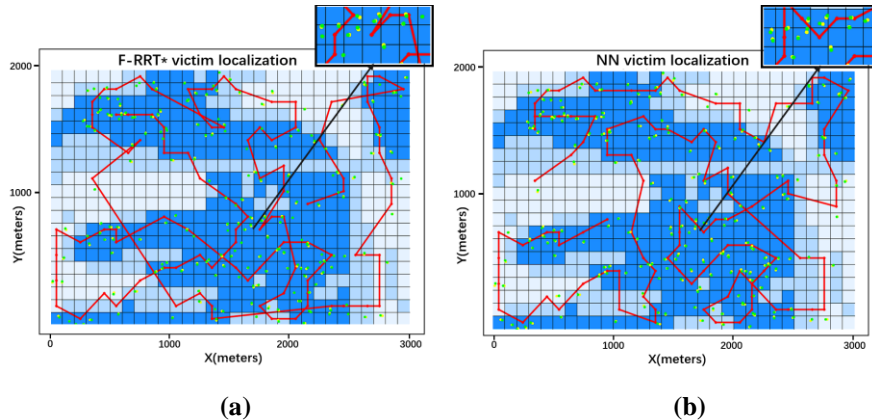


Fig. 6. System localization model comparison: (a) Disaster victim localization using the proposed F-RRT* trajectory; (b) Disaster victim localization using the comparative NN algorithm.

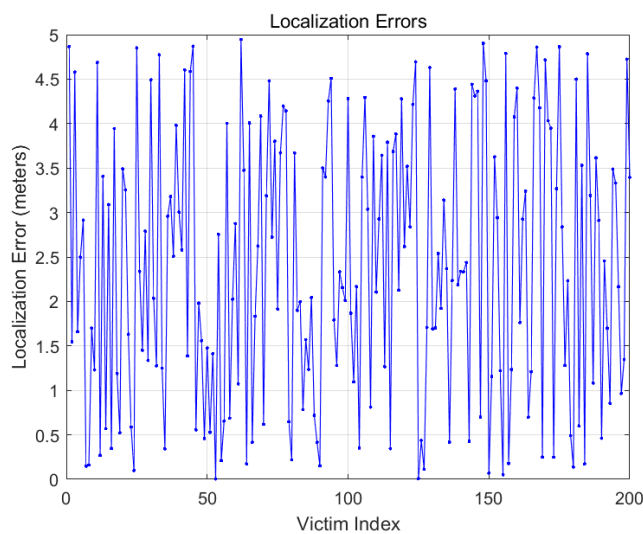


Fig. 7. Localization errors of the proposed algorithm.

4. Conclusions

This study presents an advanced UAV-based system for disaster victim localization, utilizing the Ray Tracing model and Weighted Least Squares (WLS) method for enhanced RSSI-based distance measurements. The system divides the disaster area into a grid, uses Adaptive Particle Swarm Optimization (APSO) for optimal waypoint selection, and employs the FRRT* algorithm for efficient trajectory planning.

Simulation results demonstrate that the proposed system accurately localizes disaster victims, maintaining localization errors within 5 meters. The FRRT* algorithm provides a more efficient flight path compared to the Nearest Neighbour (NN) algorithm, reducing flight costs and energy consumption. The integration of these advanced methods significantly improves disaster response efforts, ensuring swift and accurate localization of victims, thereby enhancing the speed and effectiveness of rescue operations.

Nomenclatures

D_{ij}	Disaster level at grid cell (i, j)
g	Global best position of all particles
K_{ij}	RSSI readings for grid cell (i, j)
\hat{p}	Estimated position of victim
p_i	Best position of particle i
$PL(d)$	Path loss at distance d
r_s	Signal coverage radius
$V_i(t)$	Velocity of particle i at time t
$w(t)$	Dynamic inertia weight
$x_i(t)$	Position of particle i at time t
y_{ij}	Scanning point j at grid cell i

Abbreviations

APSO	Adaptive Particle Swarm Optimization
F-RRT*	Fast-RRT*
IRRS	Integrated Received Signal Strength
RRT*	Optimized Rapid-exploring Random Trees
RSSI	Received Signal Strength Indicator
SAR	Search and Rescue
SNR	Signal-to-Noise Ratio
UAV	Unmanned Aerial Vehicle
WLS	Weighted Least Square

References

1. Zhang, R.; Li, H.; Duan, K.; You, S.; Liu, K.; Wang, F.; and Hu, Y. (2020). Automatic detection of earthquake-damaged buildings by integrating UAV oblique photography and infrared thermal imaging. *Remote Sensing*, 12(16), 2621.

2. Phang, S.K.; and Chen, X. (2021). Autonomous tracking and landing on moving ground vehicle with multi-rotor UAV. *Journal of Engineering Science and Technology*, 16(4), 2795-2815.
3. Ho, J.C.; Phang, S.K.; and Mun, H.K. (2021). 2-D UAV navigation solution with LIDAR sensor under GPS-denied environment. *Journal of Physics: Conference Series*, 2120(1), 012026.
4. Qi, J.; Song, D.; Shang, H.; Wang, N.; Hua, C.; Wu, C.; Qi, X.; and Han, J. (2016). Search and rescue rotary-wing UAV and its application to the Lushan ms 7.0 earthquake. *Journal of Field Robotics*, 33(3), 290-321.
5. Valarmathi, B.; Kshitij, J.; Dimple, R.; Srinivasa Gupta, N.; Harold Robinson, Y.; Arulkumaran, G.; and Mulu, T. (2023). Human detection and action recognition for search and rescue in disasters using yolov3 algorithm. *Journal of Electrical and Computer Engineering*, 2023(1), 5419384.
6. Saif, A.; Dimyati, K.; Noordin, K.A.; Alsamhi, S.H.; and Hawbani, A. (2024). Multi-UAV and SAR collaboration model for disaster management in B5G networks. *Internet Technology Letters*, 7(1), e310.
7. Khalil, H.; Rahman, S.U.; Ullah, I.; Khan, I.; Alghadban, A.J.; Al-Adhaileh, M.H.; Ali, G.; and El-Affendi, M. (2022). A UAV-swarm-communication model using a machine-learning approach for search-and-rescue applications. *Drones*, 6(12), 372.
8. Alhaqbani, A.; Kurdi, H.; and Youcef-Toumi, K. (2020). Fish-inspired task allocation algorithm for multiple unmanned aerial vehicles in search and rescue missions. *Remote Sensing*, 13(1), 27.
9. Oh, D.; and Han, J. (2021). Smart search system of autonomous flight UAVs for disaster rescue. *Sensors*, 21(20), 6810.
10. Dong, J.; Ota, K.; and Dong, M. (2021). UAV-based real-time survivor detection system in post-disaster search and rescue operations. *IEEE Journal on Miniaturization for Air and Space Systems*, 2(4), 209-219.
11. Phang, S.K.; Chiang, T.H.A.; Happonen, A.; and Chang, M.M.L. (2023). From satellite to uav-based remote sensing: A review on precision agriculture. *IEEE Access*, 11, 127057.
12. Demiane, F.; Sharafeddine, S.; and Farhat, O. (2020). An optimized UAV trajectory planning for localization in disaster scenarios. *Computer networks*, 179, 107378.
13. Cui, J.Q. et al. (2015). Drones for cooperative search and rescue in post-disaster situation. *Proceedings of the 2015 IEEE 7th International Conference on Cybernetics and Intelligent Systems (CIS) and IEEE Conference on Robotics, Automation and Mechatronics (RAM)*, Siem Reap, Cambodia, 167-174.
14. Cui, J.Q. et al. (2016). Search and rescue using multiple drones in post-disaster situation. *Unmanned Systems*, 04(01), 83-96.
15. Liao, B.; Wan, F.; Hua, Y.; Ma, R.; Zhu, S.; and Qing, X. (2021). F-RRT*: An improved path planning algorithm with improved initial solution and convergence rate. *Expert Systems with Applications*, 184, 115457.